Simultaneous Visualization of Multiple Gene Expression in Single Cells Using an Engineered Multicolor Reporter Toolbox and Approach of Spectral Crosstalk Correction

Jundong Han,[†,§] Aiguo Xia,[‡,§] Yajia Huang,[‡] Lei Ni,[‡] Wenhui Chen,[†] Zhenyu Jin,[†] Shuai Yang,*[,‡] and Fan Jin*[,‡,†]

[†]Hefei National Laboratory for Physical Sciences at the Microscale, Department of Polymer Science and Engineering, University of Science and Technology of China, No. 96, JinZhai Road Baohe District, Hefei, Anhui 230026, PR China

[‡]Institute of Synthetic Biology, Shenzhen Institutes of Advanced Technology, Chinese Academy of Sciences, Shenzhen 518055, PR China

S Supporting Information

ABSTRACT: Synthetic biology aims to make biology easier to engineer and focuses on the design and construction of core components that can be modeled, understood, and tuned to meet specific performance criteria, and the assembly of these smaller parts and devices into larger integrated systems to solve specific problems. Here, we designed and engineered a multicolor fluorescent reporter toolbox to simultaneously monitor the activities of multiple genes in single cells. The toolbox contained standardized and well-characterized genetic building blocks for the convenient and reproducible assembly of multiple promoter−reporter fusions (ranging from 1 to 4) into a single plasmid. Given the common problem of spectral crosstalk among multiple fluorescent proteins, we deciphered multiple spectral signatures within cells through a deduced linear unmixing algorithm. Our approach enabled the quantification of gene expression with direct FP concentrations, instead of mix-contributed fluorescence intensities, thus enabling true signal separation with high confidence. This approach performed well in the imaging of mixing cells with single FP labels. Additionally, combining with the multicolor toolbox, we succeeded in simultaneously monitoring the genetic dynamics of four selected quorum-sensing genes in response to the induction of two exogenously added autoinducers and were able to examine gene regulatory connections within the QS signaling network in *Pseudomonas aeruginosa*. Overall, this synthetic framework (*i.e.*, the genetic toolbox and the well-evaluated approach of spectral correction) will be useful for applied synthetic biology projects, multicolor imaging, and analyzing interactions of multiple genes of natural genetic networks or assembling synthetic ones.

KEYWORDS: *multicolor, gene expression, fluorescent reporter, synthetic framework*
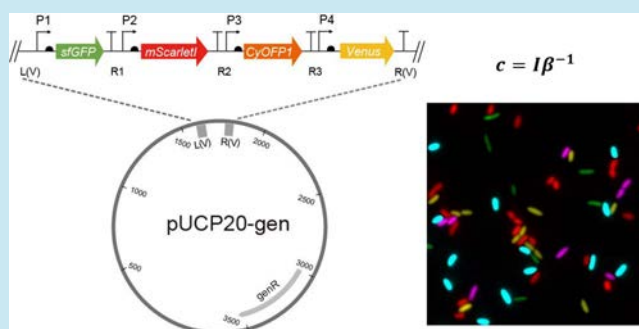
Fluorescent proteins (FPs) can be applied in a large variety of studies related to various aspects of living systems, including promoters tracking.[1] Fusing the promoter of a gene of interest to an FP as a reporter, researchers can quantify promoter activity, or corresponding gene expression, through examining the activity of the reporter.[2,3] Although plenty of methods, such as RT-qPCR,[4] RNA-Seq,[5] and enzyme-based assays, examples of which are chloramphenicol acetyl transferase (CAT), *β*-galactosidase, and luciferase,[6] are accessible to analyze gene expression, the FP-based approach has unique merits. It does not require cell lysis prior to measuring compared with RT-qPCR and RNA-seq. Fluorescent genes have lower sensitivity than enzyme-based assays, but they do not require a cofactor to function, which enables *in vivo* visualization without exogenous intervention. FP reporters also allow high temporal resolution measurement of promoter activity in living cells in a given genetic environment and in

response to an external influence, by monitoring the differentiation of fluorescent signal with respect to time.[7−9] In addition to measurements on cell populations, fluorescent reporter strains can be used to assay promoter activity in individual living cells with fluorescence microscopes.[10,11] Furthermore, the emerging development of FPs has expanded the spectrum of FPs to a full range,[12,13] showing strong promise for simultaneous measurement of promoter activities of multiple target genes.

Using multiple reporters in a cell can reveal information not obtainable from only one reporter. Cloning multiple FPs under a control of several promoters, multiple fluorescent reporters enable monitoring multiple genes simultaneously in single cells and can be further used to investigate interactions between
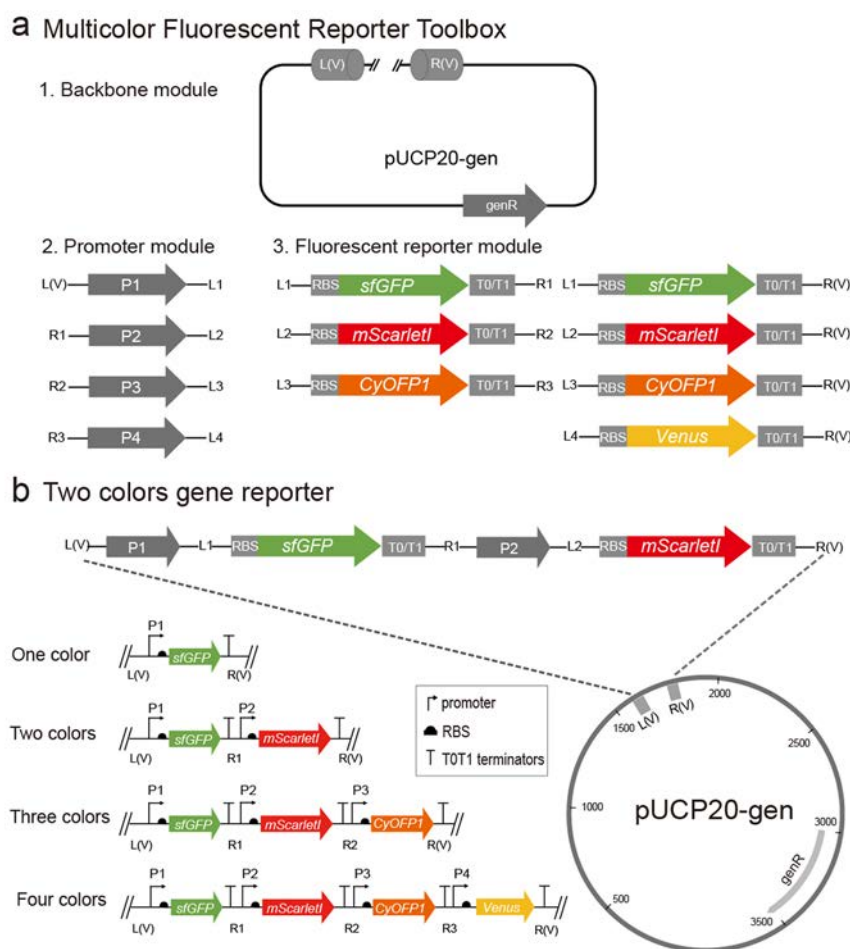
Figure 1. Design and construction of a multicolor fluorescent reporter toolbox. (a) The toolbox contained three modules, including backbone, promoter, and fluorescent reporter modules. The basic DNA parts of the toolbox were flanked with different prefixes and suffixes (L1, L2, L3, L4, L(V), R1, R2, R3, and R(V)) for the assembly of multiple promoter−reporter fusions into the backbone, where the adjacent fragments sharing terminal sequence overlaps can be jointed into a covalently sealed DNA molecule. P1−P4 represent hypothetical promoters. (b) One can construct a biosensor with multiple promoter−reporter fusions ranging from one to four color(s) using our toolbox in a single assembly reaction. An example given in the amplification picture showed the structure of a two-color gene reporter.

natural genes, or to facilitate the "debugging" of biologically engineered genetic networks. However, the application of multiple FPs for live cell imaging have been hindered by various factors. Most prominently, broad excitation and emission spectra of FPs results in spectral crosstalk among them,[12,14] limiting the ability to distinguish one signal from another with any confidence. Classically, color separation of fluorescence emission can be achieved by choosing a set of optical bandpass filters that select different parts of the emission signals.[10] Such an approach is ideal if the emission spectra of the different FPs do not overlap in the selected wavelength ranges, and is suitable for two distinct FPs, such as GFP and RFP. However, in systems where three or more FPs are used, spectral crosstalk can be difficult eliminate by purely physical means.[15−17] Notably, even a very small spectral crosstalk between two reporters would show up as a very strong correlation signature.[15] To solve this problem, several approaches for crosstalk correction have been used to enhance spectral resolution in fluorescence microscopy.[18−22] However, the slow image acquisition and the need for specialized hardware and software, respectively, for spectral scans and subsequent data processing limited the widespread use of these

methods. Thus, what is needed is an easy-to-use approach to correct the spectral crosstalk.

Here, in this study, we first described a plasmid-based platform for design and building a multicolor fluorescent reporter toolbox using synthetic biology techniques, which can be used to assemble and form a multicolor reporter (ranging from 1 to 4) as required in a single step. We then attempted to tackle the spectral crosstalk issues of five chosen FPs. The true challenge in spectral crosstalk correction of multicolor fluorescent reporters is the ability to separate the fluorescence contribution from multiple FPs. We distinguished each signal through a deduced linear unmixing algorithm based on the finding that the measured fluorescence of one specific channel is a linear spectral mixing of multiple FPs. Our established approach is versatile and easy to implement without any specialized hardware or extensive data processing. We obtained absolute FP concentrations of each pixel of the corresponding original fluorescent images using simple linear algebra, and quantified the levels of gene expression with direct FP concentrations, hence enabling true signal separation. Mixing cells with single FP labels, our correction approach performed well, yielding little or no signal from the other spectral signatures, indicated by the fact that each cell was clearly
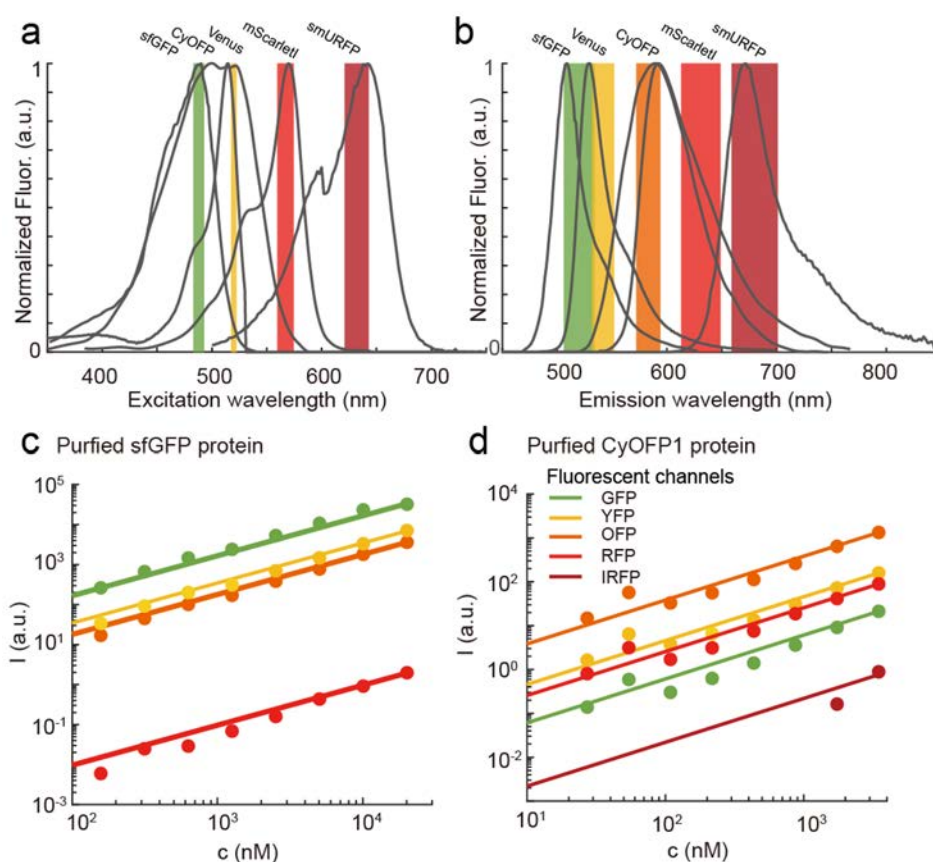
Figure 2. Spectral crosstalk among FPs. (a,b) The excitation and emission spectrum of five FPs (sfGFP, Venus, CyOFP1, mScarletI, and smURFP). The five filter sets indicated by color parts in (a) and (b) corresponded to GFP, YFP, OFP, RFP, and IRFP fluorescent channels, respectively. (c,d) The fluorescence data of purified sfGFP and CyOFP1 in all five fluorescent channels, respectively. This data showed the substantial crosstalk of sfGFP or CyOFP1 fluorescence into other channels. The fluorescence and the concentration of each FP in all channels exhibited an excellent lineal relationship, implying that the measured fluorescence of one specific fluorescent channel is a linear spectral mixing (data of other FPs were displayed in Figure S1).

defined as being either labeled or not labeled. Finally, we constructed a four-color fluorescent reporter using our newly developed toolbox to examine the genetic activities of four quorum-sensing (QS) related genes in *Pseudomonas aeruginosa* as a demonstration. We made corrections for the fluorescent images in different fluorescent channels to separate signals using our approach, and performed further analyses to examine gene regulatory connections, and obtained consistent results with previous studies.

RESULTS

Construction of Multicolor Fluorescent Reporter Toolbox. The basic design principle here is that the toolbox has the capability of providing a collection of interchangeable parts for the standardized work easily. To address this, we designed and built the multicolor fluorescent reporter toolbox with three modules, including backbone, promoter, and fluorescent reporter module (Figure 1a). The DNA fragments of these three modules can be assembled to form a biosensor with multiple promoter−reporter fusions (ranging from 1 to 4) as required using the Gibson assembly method.[23]

We employed an empty integrative vector, pUCP20-gen, as the backbone, which was constructed by replacing the original carbenicillin resistance cassettes of pUCP20[24] with gentamicin resistance markers. The replacement can enhance the utility and stability of the vectors in *P. aeruginosa* that are inherently resistant to many of the antimicrobial markers except for gentamicin.[25] The backbone was linearized and flanked with a prefix (L(V)) and suffix (R(V)) by PCR. For the design of reporter modules, we chose four fast maturing, monomeric FPs: sfGFP,[26] mScarletI,[27] CyOFP1,[28] and Venus,[29,30] and each gene of these FPs was arranged between an optimized ribosomal binding site RBSII[31] and two strong consecutive transcriptional terminators T0T1[32] as the basic construct. The same RBS of different fluorescent genes ensured the fusions that were transcribed under the control of the fused promoter but translated independently of the promoter sequences. The added strong terminators can efficiently eliminate transcriptional interference to isolate the four open reading frames (ORFs) (*i.e.*, fusions of promoters and fluorescent reporter genes) by preventing undesired read-through transcription effect from other operons. The basic reporter blocks were flanked with different prefixes (L1, L2, L3, and L4) and suffixes (R1, R2, R3, and R4) for the fusions of multiple promoter−reporter systems. The promoter module consisted of amplified promoters with the prefixes (L(V), R1, R2, and R3) and suffixes (L1, L2, L3, and L4) compatible with the backbone and the fluorescent reporter module, which enabled the assembly of different DNA fragments of these three modules.

In our design, the prefixes and suffixes, which were generated from random sequences and added by PCR through the design of PCR primers, resulted in the DNA fragments that
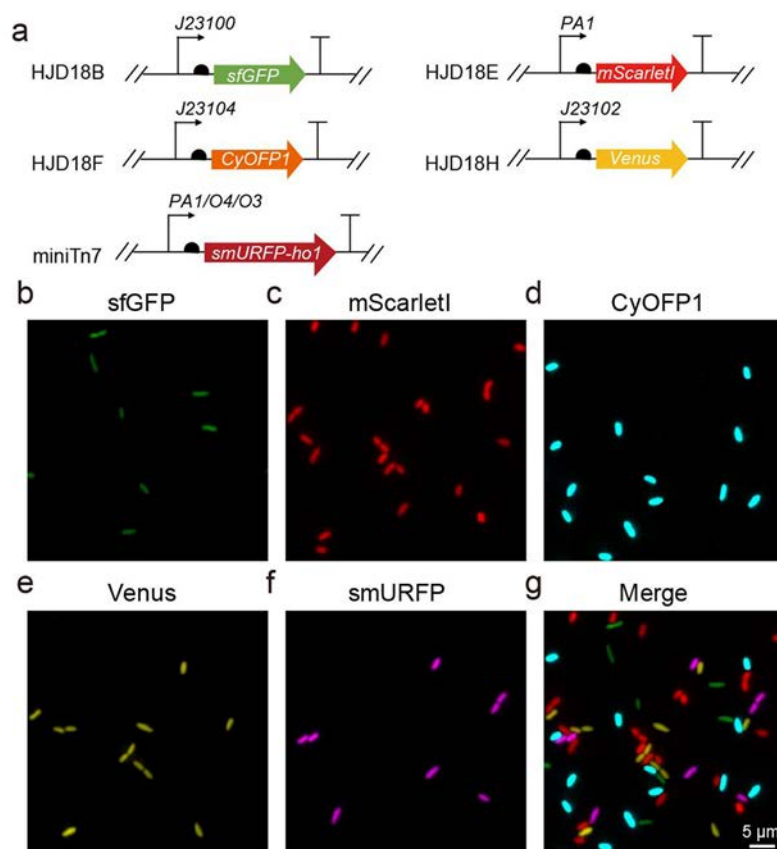
Figure 3. Signal separation of mixed cells with single labels. (a) Gene maps of each single promoter−reporter fusion. The five FP genes, *sfGFP*, *Venus*, *CyOFP1*, *mScarletI*, and *smURFP*, were expressed under the control of a series of strong constitutive promoters, *J23100*, *J23102*, *J23104*, *PA1*, and *PA1/O4/O3*. Five groups of cells, each of which expressed only a single FP, were mixed for imaging. (b−f) The converted concentration images of each FP were represented after spectral correction using our approach, where the expression levels were pseudocolored (green, yellow, cyan, red, and purple for sfGFP, Venus, CyOFP1, mScarletI, and smURFP). That the cells in each image were clearly defined as being labeled or not labeled showed good performance of our correction approach of spectral crosstalk. (g) Merged image of (b−f). Scale bar, 5 μm.

overlapped in sequence by ∼25 bases. The adjacent DNA fragments sharing terminal sequence overlaps can be joined into a covalently sealed molecule in a single Gibson reaction.[23] Taking two-color fluorescent reporters as an example, four DNA fragments with overlaps of prefixes and suffixes, including P1 promoter module, *sfGFP* module, P2 promoter module, *mScarletI* module, were sequentially joined into the linearized vector backbone pUCP20-gen to implement integrated two-color reporter plasmids using Gibson assembly.[23] Using a similar approach, a biosensor with multiple promoter−reporter fusions ranging from one to four color(s) can be easily assembled from DNA fragments with different prefixes and suffixes of our toolbox (Figure 1b, inserted panel).

Correction for Spectral Crosstalk among Five FPs. Apart from the four aforementioned FPs, we introduced a red FP, smURFP,[33] to expand fluorescence spectra to near-infrared (Figure 2a). smURFP was not involved in the design of multicolor fluorescent reporter toolboxes but used for labeling cells and segmentation of cells in the following study. Figure 2a and 2b represented the excitation and emission spectra of sfGFP, Venus, CyOFP1, mScarletI, and smURFP. We customized five sets of fluorescent filters for the excitation and collection of the fluorescent light of these five FPs, which were indicated by color parts in the excitation and emission spectra. The five filter sets corresponded to GFP, YFP, OFP, RFP, and IRFP fluorescent channels as the natural channel for

sfGFP, Venus, CyOFP1, mScarletI, and smURFP, respectively. For instance, GFP channel is the natural channel of sfGFP, and other channels, YFP, OFP, RFP, and IRFP channels, are named the crosstalk channels of sfGFP. The spectral patterns in Figure 2a and 2b demonstrated considerable spectral crosstalk; that is, a single excitation wavelength can excite more than one FP, and also the fluorescence collected from each customized filter contained intensity that were emitted by more than a single FP. We have made an appropriate choice of fluorescent filters to minimize the microscope spectral crosstalk, but cannot achieve a clean separation of the synchronous fluorescence signals from all five FPs due to close spectral overlap among them.

In order to check and correct for spectral crosstalk between FPs, we constructed plasmids containing each individual FP gene expressed on a pBAD promoter for purification (see Methods). Each purified FP was diluted to different concentrations, and its fluorescence was measured in all five fluorescent channels. We representatively demonstrated the purified protein of sfGFP plotted with its fluorescence and the corresponding concentration in all five fluorescent channels in Figure 2c. The results showed the substantial crosstalk of sfGFP fluorescence into the YFP and OFP channel, which had a magnitude close to 20% and 10% of the detection level in its natural channel (GFP channel). In comparison, the crosstalk of sfGFP into the RFP channel was low to 0.06‰, and the
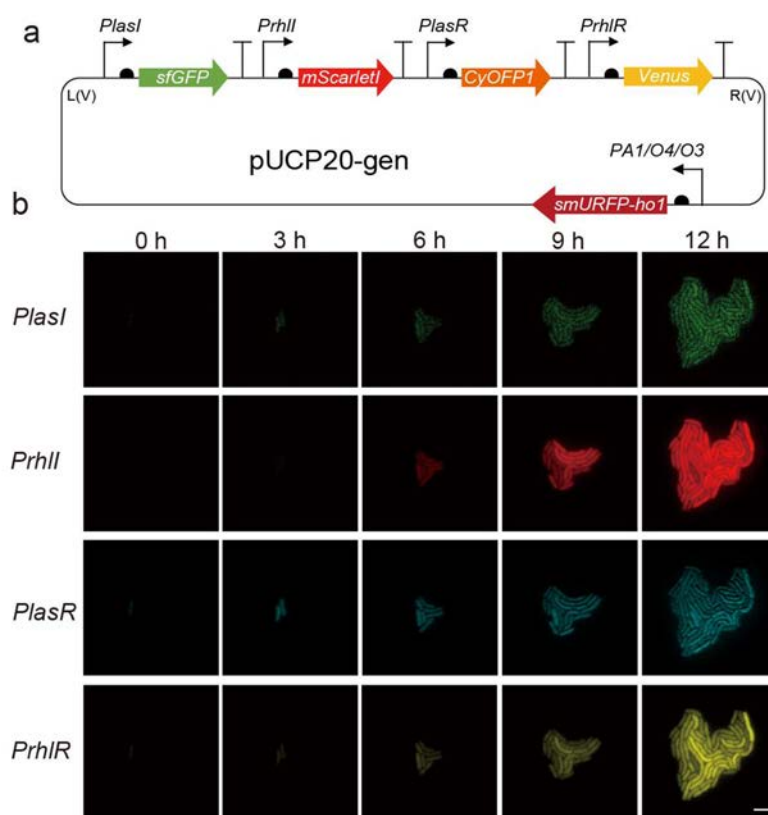
Figure 4. Simultaneous monitoring of gene expression of four quorum-sensing genes in *Pseudomonas aeruginosa*. (a) The promoter regions of *lasI*, *rhlI*, *lasR*, and *rhlR* fused to reporter genes of *sfGFP*, *mScarletI*, *cyOFP1*, and *Venus* were assembled into pUCP20-gen using our newly developed toolbox. smURFP were introduced under the control of PA1/O4/O3 for labeling cells and segmentation. Cells of JP2 (*lasI* and *rhlI* double mutations) harboring the reporter were cultured under the induction of C4-HSL and C12-HSL signal molecules (80 µM). Expression of the four QS genes were tracked in a growing microcolony with time-lapse microscopy. (b) Time-lapse images of each FP concentration distribution in a growing single-layer microcolony. Scale bar, 5 µm.

crosstalk into the IRFP channel was undetectable in our filter set. Combining with the fluorescent data of four other purified FPs, we further confirmed the spectral crosstalk (Figure 2d and Figure S1). Moreover, we found that the fluorescence and the concentration of each FP in its natural channel as well as other crosstalk channels exhibited a very good linear relationship, which implied that the measured fluorescence of one specific channel is a linear spectral mixing. Particularly, in our system, the linearly mixed fluorescence contained simultaneous emission of the five FPs; the measured fluorescence, I_j, (the subscripts, $j = a, ..., e$, refer to GFP, YFP, OFP, RFP, and IRFP channels, respectively), of any channel can be expressed as

$$[I_a I_b I_c I_d I_e] = [c_1 c_2 c_3 c_4 c_5] \begin{bmatrix} \beta_{a1} & \beta_{b1} & \beta_{c1} & \beta_{d1} & \beta_{e1} \\ \beta_{a2} & \beta_{b2} & \beta_{c2} & \beta_{d2} & \beta_{e2} \\ \beta_{a3} & \beta_{b3} & \beta_{c3} & \beta_{d3} & \beta_{e3} \\ \beta_{a4} & \beta_{b4} & \beta_{c4} & \beta_{d4} & \beta_{e4} \\ \beta_{a5} & \beta_{b5} & \beta_{c5} & \beta_{d5} & \beta_{e5} \end{bmatrix} \quad (1)$$

The subscripts ($k = 1, ...,5$) of protein concentration c_k represent FPs of sfGFP, Venus, CyOFP1, mScarletI, and smURFP, respectively. β_{jk} is the weighting coefficient of the FP k in the fluorescent channel j, which was achieved by linearly fitting the slopes of fluorescence intensities to protein concentrations. Note that β_{jk} is dependent on the choice of

filters. We listed the measured matrix value of our microscope setup in Table 2.

Given a certain fluorescent channel, such as GFP channel, the measured fluorescence I_a was described as

$$I_a = c_1 \beta_{a1} + c_2 \beta_{a2} + c_3 \beta_{a3} + c_4 \beta_{a4} + c_5 \beta_{a5} \quad (2)$$

A more general description can be written as

$$\mathbf{I} = \mathbf{c}\boldsymbol{\beta} \quad (3)$$

The measured fluorescence $\mathbf{I}$ was first normalized with respect to the exposure time and excitation laser intensity. Because the weighting matrix $\boldsymbol{\beta}$ was experimentally measured from the purified FP solution, we then corrected $\mathbf{I}$ by the ratio of the height of bacterial cells to the z-position of imaging of purified FP solution (see Methods). Finally, we can solve the concentration matrix $\mathbf{c}$ through linear algebra:

$$\mathbf{c} = \mathbf{I}\boldsymbol{\beta}^{-1} \quad (4)$$

where $\boldsymbol{\beta}^{-1}$ is the inverse matrix of $\boldsymbol{\beta}$. The elements of matrix $\mathbf{c}$ are the concentrations of each of the FPs in cells that have independence of each other, which allows for distinguishing one signal from another, enabling correction of the spectral crosstalk.

Distinguishing Five Colors in Single Images. In order to determine if we could distinguish multiple fluorescent entities from the same image using our correction approach, we mixed five groups of cells after they were individually transformed with a plasmid encoding sfGFP, Venus, CyOFP1,
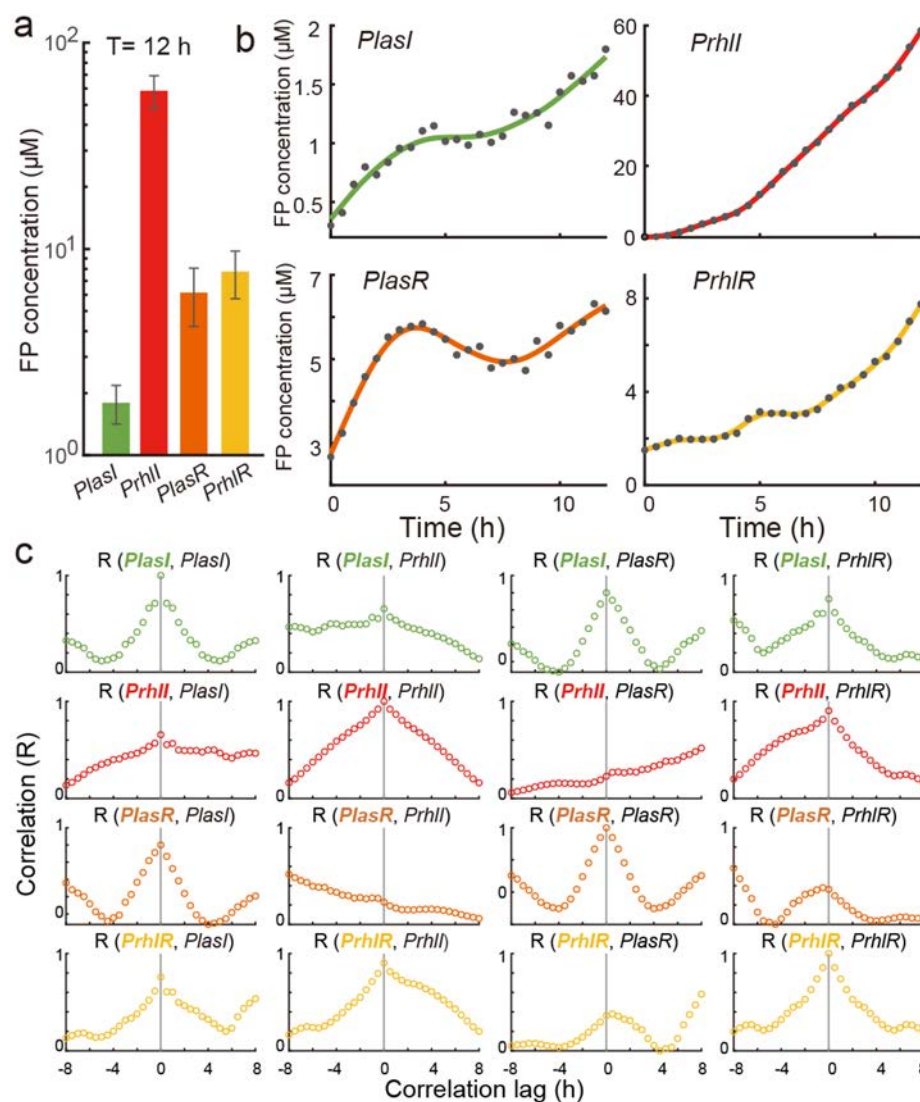
Figure 5. Analysis of genetic activities of four quorum-sensing genes. (a) Average expression levels of each quorum-sensing gene after an induction of 12 h. Error bars depict standard deviations. (b) Dynamics of gene expression. The four selected QS genes were all upregulated in response to the exogenously added autoinducers. Black dots represent the average FP concentrations of single cells at the indicated time points, and lines are the smooth data. (c) Correlations of gene expression between pairs of the four quorum-sensing genes to examine regulatory connections.

mScarletI, or smURFP, so that cells of each strain would express only a single FP. The expression of each FP was under the control of a series of strong constitutive promoters, such as J23100, J23104, J23102 (IGEM, biobricks), PA1, and PA1/O4/O3[34] (Figure 3a). The strains carrying the respective plasmid were cultured under the same conditions and mixed for imaging in different fluorescent channels (see Methods). The acquired fluorescent images were corrected for spectral crosstalk using our linear unmixing algorithm (eq 4). The fluorescent intensity of each pixel was analyzed to compute the corresponding FP concentration. The image of concentration information for each FP was created by displaying the computed concentration value of each pixel as an image, where the location of each pixel was the same with the fluorescence image. Figure 3b−f displayed the converted concentration images of each FP when the expression levels were pseudocolored (green, yellow, cyan, red, and purple for sfGFP, Venus, CyOFP1, mScarletI, and smURFP, respectively), in which each cell was clearly defined as being either labeled or not labeled. This demo showed good performance

of our algorithm for the correction of spectral crosstalk. Additionally, we merged the five FP images (Figure 3b−f) into a single image (Figure 3g). The absence of pixels with overlapping colors, such as appearing yellow (the combination of red and green), cyan (the combination of red and yellow), or other colors with any combination of the mentioned five labeling pseudocolors, in the merged image showed there was little or no signal from the other spectral signatures. In contrast, the fluorescent channel images showed some of the cells with fluorescence in two or more fluorescent channels and obvious overlapping colors in the merged image, indicating the substantial spectral crosstalk of the standard channel fluorescence images (Figure S2). Furthermore, we showed the inaccuracies caused by the spectral crosstalk informatively using a series of reporters, and found that using the fluorescent intensities to infer the corresponding promoter activities would lead to qualitatively erroneous results, and our established unmixing approach could correctly separate the mixed signals (Figure S3). Taken together, these results validated the
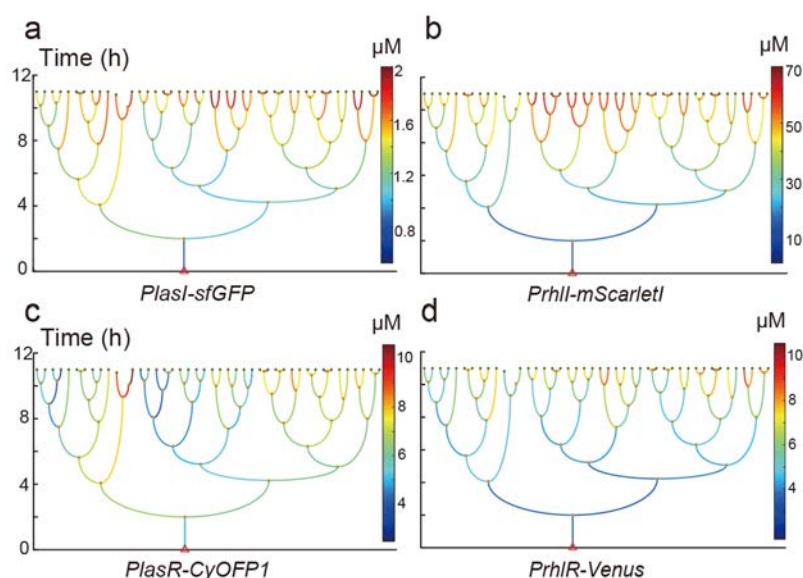
Figure 6. Construction of genealogical trees for growing cells. The genealogical tree in a growing microcolony contained the genetic activity of *lasI* (a), *rhlI* (b), *lasR* (c), and *rhlR* (d), as well as the growth information on single cells, which can be used for deep analysis.

capability and feasibility of our approach for separating emission signals of multiple FPs when used simultaneously.

Four-Color Reporter for Monitoring the Expression of Quorum-Sensing Genes. We further constructed a four-color fluorescent reporter using our newly developed toolbox to examine the genetic activities of four QS genes in *P. aeruginosa*, including *lasI*, *rhlI*, *lasR*, and *rhlR*, where the promoter regions of them controlled the fluorescent reporter genes of *sfGFP*, *mScarletI*, *CyOFP1*, and *Venus*, respectively. To ensure the response of the biosensor only in the presence of exogenously added autoinducers, N-butanoyl-L-homoserine lactone (C4-HSL) and N-(3-oxododecanoyl)-L-homoserine lactone (C12-HSL), we constructed and used strain PAO1 with *lasI* and *rhlI* double mutations (JP2) to exclude the partial effects caused by interference of the two known endogenous *P. aeruginosa* autoinducers directly synthesized by LasI and RhlI (Figure S4).[35] We also introduced the smURFP under the control of a constitutive promoter *PA1/O4/O3* as an internal control, also for labeling cells and segmentation (Figure 4a). We employed a protocol enabling seeding and growing cells on small agarose pads and imaging the resulting microcolonies.[36] Cells of JP2 carrying the biosensor were sandwiched between an agarose pad, made of 2% (wt/vol) agarose with FAB medium containing glutamate as carbon source and gentamycin to maintain the plasmid, and a cover glass, which allowed for a single layer of bacteria to form, further enabling the measurement of single-cell gene expression dynamics. The FAB agarose pad was supplemented with C4-HSL (80 μM) and C12-HSL (80 μM) for induction, and we simultaneously tracked the expression of the four QS genes in a growing microcolony with time-lapse microscopy. The time-lapse fluorescent images of the multicolor gene reporters in different fluorescent channels were calculated for signal separation through the linear unmixing algorithm (eq 4). After the correction, we directly used protein concentration to characterize the gene expression level. We demonstrated the time-lapse distribution images of each FP concentrations in a single-layer microcolony during the induction (Figure 4b) and indicated the average expression levels at the point of 12 h by computing the corresponding FP concentration of single cells in the

microcolony (Figure 5a). We showed that the four selected QS genes had low background expression levels in the 3 μM range and had little response under the conditions of the absence of inducers (Figure S4). In response to the exogenously added autoinducers, the four QS genes were all upregulated over time, especially for the expression of *rhlI* that increased more than 20-fold after 12 h, reaching to 60 μM, while the concentrations of other three genes increased to lower than 10 μM at this point (Figure 5b). For comparison, we represented the expression dynamics of the four genes characterized by the original fluorescence intensities, which were computed from the standard fluorescent channel images, to show the inaccuracies caused by spectral crosstalk (Figure S5). We then calculated correlations of gene expression between pairs of the genes. For most of the cross correlations, the asymmetric shapes of them signified that gene regulatory interactions in the QS signaling cascade are context dependent, while the cross correlation between *PlasI* and *PlasR* was symmetric, indicating that the response of *lasI* and *lasR* to signals are almost synchronous (Figure 5c). These data agreed well with the results of other studies.[37−40] We further reconstructed genealogical trees of the microcolony shown in Figure 6 using MATLAB codes developed by our lab.[41,42] The genealogical trees contained the concentrations of each FP as well as the growth information on single cells in a growing microcolony, which can be used for deep analysis, such as the relationship of gene expression between mother cells and their offspring. In general, our multicolor reporter toolbox and approach for crosstalk correction was successful in monitoring expression of several genes simultaneously, further providing an imminent means by which we could reveal regulatory connections between genes.

■ DISCUSSION

In this study, we have designed and engineered a general chassis where multiple promoters can be easily fused to multiple FP genes on a single construct, and this synthetic biology framework could enable independent and simultaneous monitoring of multiple gene expression using FP

reporters. Since the application of multiple FPs for imaging of cells shares the common problem of spectral overlap, we tackled this issue through a deduced linear unmixing algorithm, and quantified the levels of gene expression with direct FP concentrations, thereby enabling true signal separation. We have tested the performance of our approach in the imaging of mixed cells with single FP labels or single cells with five-color labels, and it worked well on both. Conclusively, we have developed a genetic toolbox for measuring dynamic gene expression in single cells using multiple FPs on the same plasmid, and our approach for the correction of spectral crosstalk enabled distinguishing each independent signal from a mixed signal with high confidence.

A traditional fluorescent reporter often contains only one promoter−reporter fusion. When one study monitored two genes, each promoter was usually in separate plasmids.[21,43] However, the use of many backbones increased the complexity of the gene expression monitoring process since the plasmids with different replication origins may have different copy numbers, and cause different growth rates of cells due in part to additives such as antibiotics necessary to maintain plasmids, both of which could result in the difference in fluorescent intensity. Consequently, monitoring the expression of multiple genes using fluorescent reports in separate plasmids may introduce inaccuracies. By contrast, our multicolor toolbox addressed the defects, and could be a useful and convenient genetic toolkit to construct a single biosensor with multiple promoter−reporter fusions.

Our multicolor toolbox contains three essential modules: backbone regions, promoter sequences, and fluorescent reporter genes (including the RBSs and terminators). We put prefix and suffix sequences to each of those blocks so that replacement of any of them is feasible. The promoter of a gene of interest would be applicable for assembly by adding prefix and suffix sequences through the design of PCR primers. It is also possible to use other FP genes as reporters when necessary. It is worth noting that when introducing new FPs, the weighting matrix β should be remeasured. Furthermore, our toolbox may be adapted to other bacterial hosts by the replacement of backbones and optimization of codons. In combination with spectral correction, the synthetic framework has the ability of simultaneously tracking activities of several promoters from natural genes or components of synthetic networks in a broad range of bacterial species.

To study natural genetic networks, multicolor reporters can be constructed in the same way as the four-color reporter of QS genes presented in this study. The activity of one or more natural promoters can be monitored and quantified at the same time. Cells harboring the multicolor reporter could be measured for quantification of changes of promoter activity in various environmental conditions to determine a particular promoter activity state. In this way, our toolbox can be used to monitor and compare multiple context-sensitive natural promoter responses within the same regulatory network to further analyze interactions of multiple natural genes. Furthermore, the multicolor toolbox will facilitate the design and optimization of synthetic networks. Synthetic biology is incredibly nonlinear and less predictable.[44] Hence, testing the modularity of specific parts of a synthetic network will enable the rational design of larger integrated systems. The characterization and interactions of engineered parts could be analyzed by inserting regulatory promoters into the framework to control expression of multiple FPs. Alternatively, monitoring

multiple promoters of an engineered network in this way can provide insight into internal variables of the system that would otherwise be unknown, such as characterization of a synthetic oscillator or a bistable genetic switch.[45,46]

Moreover, the demonstrated ability to separate signals of FPs with closely overlapping spectra now allows a large number of fluorescent probes to be coincidentally followed. Our approach of spectral correction will also be applicable in the studies of spatiotemporal protein dynamics within live bacterial cells, such as multicolor imaging of bacterial nucleoid and division proteins,[16] in addition to the monitoring activities of multiple genes described in this study. The capability to simultaneously image multiple FPs offers obvious advantages, ranging from unique following of distinct cells in a mixed population by labeling cells individually, to distinguishable tracking promoters or intracellular components tagged with FPs in single cells. Generally, the approach made substantial progress in multicolor imaging, thereby providing a significant step to decipher the multifaceted combinations and interactions that simultaneously occur during the complex signaling cascades and cellular responses that underlie biological processes.

■ METHODS

Strains and Growth Conditions. *Escherichia coli* was propagated at 37 °C in Luria−Bertani (LB) broth or LB agar supplied with antibiotics. *P. aeruginosa* was grown on LB agar plates at 37 °C overnight, and one monoclonal colony was inoculated into a 5 mL polystyrene culturing tube containing 1 mL of minimal medium (FAB) with 30 mM glutamate as the carbon resource. Then cubes were placed into a shaking incubator at 37 °C with 220 rpm. The culture media contained antibiotics for selection at each concentration: for *E. coli*, kanamycin at 30 μg/mL, carbenicillin 100 μg/mL, gentamicin 15 μg/mL; for *P. aeruginosa*, carbenicillin at 300 μg/mL and gentamicin at 30 μg/mL. C4-HSL and C12-HSL (Sigma-Aldrich) were added to FAB medium or agarose pads with the final concentration of 80 μM to induce the quorum-sensing of JP2-HJD17C cells.

BL21-DE3 with FP expression plasmid were cultured in 5 mL LB broth at 37 °C overnight as primary culture. The bacterial cultures were further diluted (1:100) in fresh LB medium to culture to the OD_{600} of 0.5. Expression of FP was induced by the addition of 0.5 mM IPTG, and the cells were then cultured for 4 h before harvest.

Plasmids and Strains Construction. The plasmids and bacterial strains in this study were listed in Table S1, and the primers used were listed in Table S2. The coding sequences of FPs (sfGFP, mScarletI, CyOFP1, Venus, smURFP) were amplified by PCR and ligated to pET28a for purification. Then the plasmids (HJD13A, HJD13F, HJD13H, HJD13I, and HJD13J) were obtained and transformed to BL21-DE3. The plasmids, including HJD17C, HJD18B, HJD18E, HJD18F, and HJD18H, were constructed using our multicolor fluorescent reporter toolbox and introduced into *P. aeruginosa* or its mutants by electric transformation.

JP2 was obtained from wild-type PAO1 by knocking out the genes of *lasI* (*PA1432*) and *rhlI* (*PA3476*) using well-established protocols based on two-step allelic exchange.[47] HJD14A and HJD14C were constructed for *lasI* and *rhlI* deletions. Mutants were confirmed by PCR and sequencing. Mini-Tn7 system used in this study was employed for inserting genes into the genome of *P. aeruginosa*.[32]

FP Purification. FP genes were expressed on a pBAD vector (HJD13A, HJD13F, HJD13H, HJD13I, HJD13J) with a polyhistidine tag on the C terminus. Cells were lysed using ultrasonication, and FPs were purified using Ni-NTA column (Invitrogen) purification. The purified FPs were eluted by adding the elution buffer (Sangon), and the absolute concentration was measured by the Pierce BCA Protein Assay Kit (ThermoFisher).

Microscopy. Fluorescent images were obtained using an invert fluorescent microscope (IX-71 Olympus) equipped with a 100× oil objective (Olympus), an automated xy-stage (Ludl), and two sCMOS cameras (Zyla 4.2, Andor). A solid-state light source with tunable color bands (Lumencor Spectra X) and customized emission bandpass filters were respectively used for excitation and collecting fluorescent light, where the information on filters were included in Table 1. Note that

Table 1. Fluorescent Filters

FP	sfGFP	CyOFP1	Venus	mScarletI	smURFP
excitation filter (nm)	488/10	488/10	520/5	567/15	632/22
emission filter (nm)	520/28	583/22	542/20	631/36	680/42
filter cube[a,b]	cube 1	cube 1	cube 2	cube 1	cube 1

[a]Filter cube 1: FF409/493/573/652 (Semrock), FF01-432/515/595/730 (Semrock). [b]Filter cube 2: FF459/526/596 (Semrock), FF01-475/543/702 (Semrock).

the same light excited sfGFP and CyOFP1, but the emission lights were separately received into two cameras through the separation of a dichroic mirror 552 nm (Semrock). Microscope control was done with MATLAB (MathWorks) scripts interfacing with μManager.[48] Frame rate of acquired fluorescent images was dependent on bacterial density (5−15 min/frame), and exposure time was low (50−100 ms) to reduce photobleaching.

Time-Lapse Experiment. JP2 cells containing the plasmid HJD17C were grown overnight in FAB medium supplied with 30 mM glutamate and 30 μg/mL gentamicin. The bacterial cultures were then diluted 100× into fresh FAB medium to culture to the OD_{600} of 0.6. The resultant cells were further suspended into fresh FAB to an OD_{600} of ~0.02 for use. After loading the suspended cells on the top of an agarose pad (containing 30 mM glutamate, 30 μg/mL gentamicin, 80 μM C4-HSL and C12-HSL), the pad was flipped and transferred to an imaging dish.[36] Time-lapse images were acquired at 30 min intervals in a 28 °C temperature-controlled chamber.

Fluorescence Characterization and Image Processing. Each purified FP solution was diluted to different concentrations of 0.03−20 μM with PBS buffer, and added into a cover glass-bottom dish for the measurement of fluorescence. The intensities were measured in all five

fluorescent channels at the z-position of 80 μm apart from the glass surface. The measured fluorescence was normalized with respect to the exposure time and excitation laser intensity. Each FP was plotted with the concentrations on the x-axis and the normalized intensities of different fluorescent channels on the y-axis for linear fitting, and the measured weighting matrix β of our setup was listed in Table 2.

The fluorescent microscopy images of bacterial cells were subjected to image segmentation and single-cell tracking using MATLAB programs developed by us.[41,42] In brief, image segmentation was done using images from the bright, constitutively expressed (PA1/O4/O3 promoter) smURFP. The edges of cells were detected using the Laplacian of Gaussian method. The background fluorescence was first corrected by the excitation image of a net coverslip, which allowed the direct reflection of a portion of excitation light to camera. Then, the fluorescent intensity of each pixel was calibrated by the ratio of the height of bacterial cells to the z-position of imaging of purified FP solution, both of which were determined using the z-axis scan of microscopy. We assumed that the thickness of FP solution is proportional to the fluorescence intensity when the thickness is small enough, and thus the intensity can be corrected by the height ratio. The corrected fluorescent intensity was finally analyzed to compute the corresponding FP concentration using eq 4. The gene expression level of single cells was determined directly by measuring averaged concentration values of the pixels enclosed by bacterial contours. The obtained concentration data are the absolute FP expression level, and allow for analysis and comparison of the results that are obtained from different microscope setups. Particularly, the height correction is not a necessary step if one is interested in looking at relative, rather than absolute, expression of the fluorescent proteins in the cells on a specific microscope. For the time-lapse correlation of gene expression in the QS experiment, we focused on the change of expression levels, and the differences of expression data between adjacent time points were calculated to perform correlations using the function "xcorr.m" in MATLAB R2018b.

■ ASSOCIATED CONTENT

Ⓢ Supporting Information

The Supporting Information is available free of charge on the ACS Publications website at DOI: 10.1021/acssyn-bio.9b00223.

Table S1: Bacterial strains and plasmids; Table S2: Oligonucleotides; Figure S1: Fluorescence characterization of purified FPs, mScarletI, Venus, and smURFP, in all fluorescent channels; Figure S2: Standard fluorescent images of mixed cells tagged with single FP in five fluorescent channels; Figure S3: Fluorescence inaccuracies caused by the spectral crosstalk among FPs; Figure S4: Genes of *lasI*, *rhlI*, *lasR*, and *rhlR* of JP2 cells

Table 2. Weighting Coefficient of Each FP in Different Fluorescent Channels

	channel				
FP	GFP	YFP	OFP	RFP	IRFP
sfGFP	1.67	3.35	0.18	9.60×10^{-5}	0
Venus	1.72	2.66	0.46	6.60×10^{-4}	9.80×10^{-6}
CyOFP1	6.10×10^{-3}	4.60×10^{-2}	0.38	2.6×10^{-2}	2.20×10^{-4}
mScarletI	3.70×10^{-2}	6.00×10^{-3}	0.26	0.73	5.80×10^{-3}
smURFP	2.70×10^{-5}	1.90×10^{-5}	2.10×10^{-5}	1.30×10^{-5}	0.17

only respond to the exogenously added autoinducers; Figure S5: Expression dynamics of the four genes characterized by the original fluorescence intensities computed from standard fluorescent channel images (PDF)

AUTHOR INFORMATION

Corresponding Authors

*Tel.: +86-551-6360-6925. Fax: +86-551-6360-6743. E-mail: yssamber@mail.ustc.edu.cn (S.Y.).

*Tel.: +86-551-6360-6925. Fax: +86-551-6360-6743. E-mail: fjinustc@ustc.edu.cn (F.J.).

ORCID

Zhenyu Jin: 0000-0003-2733-867X

Shuai Yang: 0000-0001-8325-4994

Fan Jin: 0000-0003-2313-0388

Author Contributions

§Jundong Han and Aiguo Xia contributed equally to this article. We are responsible for performing the study as follows: conceptualization, Fan Jin; methodology, Jundong Han, Aiguo Xia, Shuai Yang, Zhenyu Jin; investigation, Jundong, Han, Aiguo Xia, Shuai Yang, Yajia Huang, Wenhui Chen, Lei Ni; writing (original draft), Shuai Yang; writing (review and editing), Shuai Yang, Fan Jin.

Notes

The authors declare no competing financial interest.

REFERENCES

(1) Chudakov, D. M., Matz, M. V., Lukyanov, S., and Lukyanov, K. A. (2010) Fluorescent Proteins and Their Applications in Imaging Living Cells and Tissues. *Physiol. Rev. 90*, 1103−1163.

(2) Chalfie, M., Tu, Y., Euskirchen, G., Ward, W. W., and Prasher, D. C. (1994) Green fluorescent protein as a marker for gene expression. *Science 263*, 802.

(3) Plautz, J. D., Day, R. N., Dailey, G. M., Welsh, S. B., Hall, J. C., Halpain, S., and Kay, S. A. (1996) Green fluorescent protein and its derivatives as versatile markers for gene expression in living *Drosophila melanogaster*, plant and mammalian cells. *Gene 173*, 83−87.

(4) Heid, C. A., Stevens, J., Livak, K. J., and Williams, P. M. (1996) Real time quantitative PCR. *Genome Res. 6*, 986−994.

(5) Ramsköld, D., Kavak, E., and Sandberg, R. (2012) How to analyze gene expression using RNA-sequencing data, in *Next Generation Microarray Bioinformatics*, pp 259−274, Springer.

(6) Pardy, K. (1993) Reporter Enzyme Assays, in *Transgenesis Techniques: Principles and Protocols* (Murphy, D., and Carter, D. A., Eds.), pp 419−424, Humana Press, Totowa, NJ.

(7) Zaslaver, A., Mayo, A. E., Rosenberg, R., Bashkin, P., Sberro, H., Tsalyuk, M., Surette, M. G., and Alon, U. (2004) Just-in-time transcription program in metabolic pathways. *Nat. Genet. 36*, 486−491.

(8) Ronen, M., Rosenberg, R., Shraiman, B. I., and Alon, U. (2002) Assigning numbers to the arrows: parameterizing a gene regulation network by using accurate expression kinetics. *Proc. Natl. Acad. Sci. U. S. A. 99*, 10555−10560.

(9) Zaslaver, A., Bren, A., Ronen, M., Itzkovitz, S., Kikoin, I., Shavit, S., Liebermeister, W., Surette, M. G., and Alon, U. (2006) A comprehensive library of fluorescent transcriptional reporters for *Escherichia coli*. *Nat. Methods 3*, 623.

(10) Lichtman, J. W., and Conchello, J.-A. (2005) Fluorescence microscopy. *Nat. Methods 2*, 910.

(11) Ueno, T., and Nagano, T. (2011) Fluorescent probes for sensing and imaging. *Nat. Methods 8*, 642−645.

(12) Cranfill, P. J., Sell, B. R., Baird, M. A., Allen, J. R., Lavagnino, Z., de Gruiter, H. M., Kremers, G.-J., Davidson, M. W., Ustione, A., and Piston, D. W. (2016) Quantitative assessment of fluorescent proteins. *Nat. Methods 13*, 557.

(13) Dedecker, P., De Schryver, F. C., and Hofkens, J. (2013) Fluorescent proteins: shine on, you crazy diamond. *J. Am. Chem. Soc. 135*, 2387−2402.

(14) Shaner, N. C., Steinbach, P. A., and Tsien, R. Y. (2005) A guide to choosing fluorescent proteins. *Nat. Methods 2*, 905−909.

(15) Cox, R. S., Dunlop, M. J., and Elowitz, M. B. (2010) A synthetic three-color scaffold for monitoring genetic regulation and noise. *J. Biol. Eng. 4*, 10.

(16) Wu, F., Van Rijn, E., Van Schie, B. G. C., Keymer, J. E., and Dekker, C. (2015) Multi-color imaging of the bacterial nucleoid and division proteins with blue, orange, and near-infrared fluorescent proteins. *Front. Microbiol. 6*, 607.

(17) Zhang, C., Parrello, D., Brown, P. J. B., Wall, J. D., and Hu, Z. (2018) A novel whole-cell biosensor of *Pseudomonas aeruginosa* to monitor the expression of quorum sensing genes. *Appl. Microbiol. Biotechnol. 102*, 6023−6038.

(18) Lansford, R., Bearman, G. H., and Fraser, S. E. (2001) Resolution of multiple GFP color variants and dyes using two-photon microscopy and imaging spectroscopy. *J. Biomed. Opt. 6*, 311−318.

(19) Dickinson, M. E., Bearman, G., Tille, S., Lansford, R., and Fraser, S. E. (2001) Multi-spectral imaging and linear unmixing add a whole new dimension to laser scanning fluorescence microscopy. *BioTechniques 31*, 1272.

(20) Zimmermann, T., Rietdorf, J., Girod, A., Georget, V., and Pepperkok, R. (2002) Spectral imaging and linear un-mixing enables improved FRET efficiency with a novel GFP2−YFP FRET pair. *FEBS Lett. 531*, 245−249.

(21) Parrello, D., Mustin, C., Brie, D., Miron, S., and Billard, P. (2015) Multicolor Whole-Cell Bacterial Sensing Using a Synchronous Fluorescence Spectroscopy-Based Approach. *PLoS One 10*, No. e0122848.

(22) Xu, H., and Rice, B. W. (2009) In-vivo fluorescence imaging with a multivariate curve resolution spectral unmixing technique. *J. Biomed. Opt. 14*, 064011.

(23) Gibson, D. G., Young, L., Chuang, R.-Y., Venter, J. C., Hutchison, C. A., III, and Smith, H. O. (2009) Enzymatic assembly of DNA molecules up to several hundred kilobases. *Nat. Methods 6*, 343.

(24) Schweizer, H. P. (1991) *Escherichia-Pseudomonas* shuttle vectors derived from pUC18/19. *Gene 97*, 109−112.

(25) West, S. E. H., Schweizer, H. P., Dall, C., Sample, A. K., and Runyen-Janecky, L. J. (1994) Construction of improved *Escherichia-Pseudomonas* shuttle vectors derived from pUC18/19 and sequence of the region required for their replication in *Pseudomonas aeruginosa*. *Gene 148*, 81−86.

(26) Pedelacq, J.-D., Cabantous, S., Tran, T., Terwilliger, T. C., and Waldo, G. S. (2006) Engineering and characterization of a superfolder green fluorescent protein. *Nat. Biotechnol. 24*, 79−88.

(27) Bindels, D. S., Haarbosch, L., van Weeren, L., Postma, M., Wiese, K. E., Mastop, M., Aumonier, S., Gotthard, G., Royant, A., Hink, M. A., and Gadella, T. W. J., Jr (2017) mScarlet: a bright monomeric red fluorescent protein for cellular imaging. *Nat. Methods 14*, 53.

(28) Chu, J., Oh, Y., Sens, A., Ataie, N., Dana, H., Macklin, J. J., Laviv, T., Welf, E. S., Dean, K. M., Zhang, F., Kim, B. B., Tang, C. T., Hu, M., Baird, M. A., Davidson, M. W., Kay, M. A., Fiolka, R., Yasuda, R., Kim, D. S., Ng, H.-L., and Lin, M. Z. (2016) A bright cyan-excitable orange fluorescent protein facilitates dual-emission micros-copy and enhances bioluminescence imaging *in vivo*. *Nat. Biotechnol. 34*, 760.

(29) Griesbeck, O., Baird, G. S., Campbell, R. E., Zacharias, D. A., and Tsien, R. Y. (2001) Reducing the environmental sensitivity of

yellow fluorescent protein. Mechanism and applications. *J. Biol. Chem.* 276, 29188−29194.

(30) Shaner, N. C., Campbell, R. E., Steinbach, P. A., Giepmans, B. N. G., Palmer, A. E., and Tsien, R. Y. (2004) Improved monomeric red, orange and yellow fluorescent proteins derived from *Discosoma sp.* red fluorescent protein. *Nat. Biotechnol.* 22, 1567.

(31) Rybtke, M. T., Borlee, B. R., Murakami, K., Irie, Y., Hentzer, M., Nielsen, T. E., Givskov, M., Parsek, M. R., and Tolker-Nielsen, T. (2012) Fluorescence-Based Reporter for Gauging Cyclic Di-GMP Levels in *Pseudomonas aeruginosa. Appl. Environ. Microbiol.* 78, 5060.

(32) Choi, K.-H., and Schweizer, H. P. (2006) mini-Tn7 insertion in bacteria with single attTn7 sites: example *Pseudomonas aeruginosa. Nat. Protoc.* 1, 153−161.

(33) Rodriguez, E. A., Tran, G. N., Gross, L. A., Crisp, J. L., Shu, X., Lin, J. Y., and Tsien, R. Y. (2016) A far-red fluorescent protein evolved from a *cyanobacterial phycobiliprotein. Nat. Methods* 13, 763.

(34) Lanzer, M., and Bujard, H. (1988) Promoters largely determine the efficiency of repressor action. *Proc. Natl. Acad. Sci. U. S. A.* 85, 8973−8977.

(35) Pesci, E. C., Pearson, J. P., Seed, P. C., and Iglewski, B. H. (1997) Regulation of las and rhl quorum sensing in *Pseudomonas aeruginosa. J. Bacteriol.* 179, 3127.

(36) Young, J. W., Locke, J. C. W., Altinok, A., Rosenfeld, N., Bacarian, T., Swain, P. S., Mjolsness, E., and Elowitz, M. B. (2012) Measuring single-cell gene expression dynamics in bacteria using fluorescence time-lapse microscopy. *Nat. Protoc.* 7, 80−88.

(37) Gambello, M. J., and Iglewski, B. H. (1991) Cloning and characterization of the *Pseudomonas aeruginosalasR* gene, a transcriptional activator of elastase expression. *J. Bacteriol.* 173, 3000−3009.

(38) Latifi, A., Foglino, M., Tanaka, K., Williams, P., and Lazdunski, A. (1996) A hierarchical quorum-sensing cascade in *Pseudomonas aeruginosa* links the transcriptional activators LasR and RhIR (VsmR) to expression of the stationary-phase sigma factor RpoS. *Mol. Microbiol.* 21, 1137−1146.

(39) McKnight, S. L., Iglewski, B. H., and Pesci, E. C. (2000) The *Pseudomonas* quinolone signal regulates rhl quorum sensing in *Pseudomonas aeruginosa. J. Bacteriol.* 182, 2702−2708.

(40) Pearson, J. P., Gray, K. M., Passador, L., Tucker, K. D., Eberhard, A., Iglewski, B. H., and Greenberg, E. P. (1994) Structure of the autoinducer required for expression of *Pseudomonas aeruginosa* virulence genes. *Proc. Natl. Acad. Sci. U. S. A.* 91, 197−201.

(41) Pu, L., Yang, S., Xia, A., and Jin, F. (2018) Optogenetics Manipulation Enables Prevention of Biofilm Formation of Engineered *Pseudomonas aeruginosa* on Surfaces. *ACS Synth. Biol.* 7, 200−208.

(42) Yang, S., Cheng, X., Jin, Z., Xia, A., Ni, L., Zhang, R., and Jin, F. (2018) Differential Production of Psl in Planktonic Cells Leads to Two Distinctive Attachment Phenotypes in *Pseudomonas aeruginosa. Appl. Environ. Microbiol.* 84, e00700-18.

(43) Ravikumar, S., Ganesh, I., Yoo, I.-k., and Hong, S. H. (2012) Construction of a bacterial biosensor for zinc and copper and its application to the development of multifunctional heavy metal adsorption bacteria. *Process Biochem.* 47, 758−765.

(44) Andrianantoandro, E., Basu, S., Karig, D. K., and Weiss, R. (2006) Synthetic biology: new engineering rules for an emerging discipline. *Mol. Syst. Biol.*, DOI: 10.1038/msb4100073.

(45) Potvin-Trottier, L., Lord, N. D., Vinnicombe, G., and Paulsson, J. (2016) Synchronous long-term oscillations in a synthetic gene circuit. *Nature* 538, 514.

(46) Lou, C., Liu, X., Ni, M., Huang, Y., Huang, Q., Huang, L., Jiang, L., Lu, D., Wang, M., Liu, C., Chen, D., Chen, C., Chen, X., Yang, L., Ma, H., Chen, J., and Ouyang, Q. (2010) Synthesizing a novel genetic sequential logic circuit: a push-on push-off switch. *Mol. Syst. Biol.* 6, 350.

(47) Hmelo, L. R., Borlee, B. R., Almblad, H., Love, M. E., Randall, T. E., Tseng, B. S., Lin, C., Irie, Y., Storek, K. M., Yang, J. J., Siehnel, R. J., Howell, P. L., Singh, P. K., Tolker-Nielsen, T., Parsek, M. R., Schweizer, H. P., and Harrison, J. J. (2015) Precision-engineering the *Pseudomonas aeruginosa* genome with two-step allelic exchange. *Nat. Protoc.* 10, 1820.

(48) Edelstein, A., Amodaj, N., Hoover, K., Vale, R., and Stuurman, N. (2010) Computer control of microscopes using μManager. *Curr. Protoc. Mol. Biol.*, Unit14.20.